

# Incorporation of graphene oxide to metal-free phthalocyanine through hydrogen bonding for optoelectronic applications: An experimental and computational study

Ebru Yabaş<sup>1</sup> | Ebru Şenadım-Tüzemen<sup>2,3</sup> | Savaş Kaya<sup>4</sup> | Michael M. Maslov<sup>5</sup> | Fuat Erden<sup>6</sup>

<sup>1</sup>Advanced Technology Application and Research Center, Sivas Cumhuriyet University, Sivas, Turkey

<sup>2</sup>Faculty of Science, Department of Physics, Sivas Cumhuriyet University, Sivas, Turkey

<sup>3</sup>Nanophotonics Research and Application Center, Sivas Cumhuriyet University, Sivas, Turkey

<sup>4</sup>Health Services Vocational School, Department of Pharmacy, Sivas Cumhuriyet University, Sivas, Turkey

<sup>5</sup>Nanoengineering in Electronics, Spintronics and Photonics Institute, National Research Nuclear University, Moscow, Russia

<sup>6</sup>Department of Aeronautical Engineering, Sivas University of Science and Technology, Sivas, Turkey

## Correspondence

Ebru Yabaş, Advanced Technology Application and Research Center, Sivas Cumhuriyet University, 58140, Sivas, Turkey.

Email: [eyabas@cumhuriyet.edu.tr](mailto:eyabas@cumhuriyet.edu.tr)

Fuat Erden, Sivas University of Science and Technology, Department of Aeronautical Engineering, 58140, Sivas, Turkey.

Email: [fuaterden@sivas.edu.tr](mailto:fuaterden@sivas.edu.tr)

## Abstract

This paper focuses on incorporation of graphene oxide (GO) to metal-free phthalocyanine (MPc) through only hydrogen bonding and  $\pi$ - $\pi$  stacking. Briefly, Pc-GO composites at various concentrations were prepared by self-assembly method. The processing time was kept below 10 min to avoid covalent attachment and we aimed at answering the research question of what will happen if the conjugation is realized only through hydrogen bonding under extremely limited processing times. The as-prepared MPc-GO composites were characterized by Fourier transform infrared (FT-IR), UV-Vis, scanning electron microscope (SEM), and fluorescence analysis. We report that the interaction between MPc and GO could immediately be initiated upon mixing of corresponding solutions. Also, complete conjugation by hydrogen bonding and  $\pi$ - $\pi$  stacking could be reached even only in 5 min of sonication time. In addition, it was also determined that the prepared MPc-GO composites are stable at room conditions and during dilution. Finally, the optoelectronic properties of MPc and MPc-GO composites were also investigated experimentally and theoretically. Both experimental and theoretical results suggest that MPc-GO composites exhibit improved optoelectronic properties as compared to MPc, even though the conjugation of GO to MPc was only via hydrogen bonding without covalent attachment.

## KEYWORDS

band gap, density functional theory, graphene oxide, hydrogen bonding, phthalocyanine

## 1 | INTRODUCTION

Phthalocyanine (Pc) and Pc derivatives are widely used in optoelectronic applications due to their semiconductor characteristics, excellent thermal and chemical stability, controllable solubility, compatibility with flexible

substrates, and ease in processability.<sup>[1–3]</sup> Importantly,  $\pi$ - $\pi$  stacking in Pc structures as well as ease in judicial tuning of Pc molecules could help to realize an efficient charge transfer. Besides, Pc and Pc derivatives can form  $\pi$ - $\pi$  stacking with C-based low dimensional materials, which allows further improvement of optoelectronic

properties through introduction of C-based nanomaterials. Accordingly, composites of Pc with carbon nanotubes (CNTs), graphene (G), and graphene oxide (GO) are also widely studied to make advantage of high surface area as well as excellent physical and mechanical properties of carbon nanomaterials.<sup>[4–6]</sup>

Among these composite systems, composites of Pc with GO are receiving a special interest due to oxygen-containing functional groups on the surface and edges of GO.<sup>[7,8]</sup> Obviously, these functional groups could allow conjugation of Pc and GO via covalent attachment, electrostatic interactions, and hydrogen bonding. In this context, Zhu et al. prepared ZnPc-GO composites through a 3-day-long solution process at 130°C under nitrogen atmosphere and reported an improved nonlinear optical (NLO) extinction coefficient and broadband optical limiting performance.<sup>[9]</sup> In another work, ZnPc-GO hybrids were prepared by Song et al. through a 4-day-long solution process at room temperature and the resultant composites provided better optical limitation performance than individual GO and ZnPc.<sup>[10]</sup> Likewise, Jiang et al. prepared ZnPc-GO-hybrids by a 7-day-long solution process at room temperature and reported enhanced NLO properties.<sup>[11]</sup>

In fact, numerous different Pc molecules were designed so far, and their composites with GO were extensively studied with a particular focus on resultant optoelectronic properties. In majority of those research, conjugation of Pcs and GO were realized through covalent bonding, which actually necessitates prolonged processing times. Only a limited number of studies focused on what will happen if the conjugation is maintained by  $\pi$ - $\pi$  stacking.<sup>[12]</sup> In this context, Markad et al. used unsubstituted Pc to realize conjugation between Pc and GO through only  $\pi$ - $\pi$  stacking, and reported a slightly improved optoelectronic performance.<sup>[12]</sup> However, the research question of “what will happen if the conjugation is realized only through hydrogen bonding (in addition to  $\pi$ - $\pi$  stacking) under extremely limited processing times” still remains unanswered. Accordingly, the present work aims at answering this question through incorporation of GO to imidazole substituted metal-free Pc (MPc) via only 1–10 min of sonication process and a detailed characterization of the structural, morphological, and optoelectronic properties of the resultant MPc-GO composites. We report that conjugation through hydrogen bonding and  $\pi$ - $\pi$  stacking without covalent attachment could be realized in 5 min as verified by Fourier transform infrared (FT-IR), UV-Vis, scanning electron microscope (SEM), and fluorescence analysis. Besides, further sonication beyond this point was found to be providing no structural and morphological changes, and thus, suggesting 5 min is enough for complete conjugation. Also, the

optoelectronic properties of the resultant MPc and MPc-GO composites were studied both experimentally and theoretically. In this context, UV-Vis and fluorescence spectroscopy results suggest improved NLO properties in MPc-GO composites. Also, the band gap of the MPc-9 wt.%GO composites ( $\sim$ 1.57 eV) were found to be about 10% lower than MPc by using Tauc plot, thus, the MPc-GO composites could absorb more photons from solar radiation and could provide higher energy yield. These observations were also verified by theoretical predictions.

## 2 | EXPERIMENTAL

### 2.1 | Synthesis of MPc and MPc-GO composites

MPc was prepared as detailed in our previous work.<sup>[13]</sup> In a regular synthesis procedure, 4-nitrophthalonitrile was mixed with 4,5-diphenylimidazolethiol in a basic medium to prepare phthalonitrile. Then, MPc was synthesized by tetramerization reaction of as-prepared phthalonitrile in DMF. For the preparation of MPc-GO composites, various amounts of GO were dispersed in a 5-mL DMSO solution (MPc-GO-1: 0.0001  $\mu$ g/mL GO, MPc-GO-2: 0.001  $\mu$ g/mL GO, MPc-GO-3: 0.01  $\mu$ g/mL GO, MPc-GO-4: 0.05  $\mu$ g/mL GO, MPc-GO-5: 0.1  $\mu$ g/mL GO, MPc-GO-6: 1  $\mu$ g/mL GO). In a separate beaker, MPc was also dispersed in a 5-mL DMSO at a concentration of 10  $\mu$ g/mL. These solutions were then mixed and immediately sonicated at 750 W ultrasound power for different times by a Sonics VCX-750 Vibra Cell ultrasonic homogenizer. Finally, the sonication products were washed and filtered, and then dried at 50°C in vacuum oven.

### 2.2 | Characterization

The absorption and fluorescence spectra were recorded on a Shimadzu UV-1800 spectrophotometer and Agilent Cary Eclipse G9800A Fluorescence Spectrometer, respectively. The FT-IR spectra was recorded on a Bruker Tensor II-ATR. The morphology of MPc-GO composites were studied by a TESCAN MIRA 3 XMU SEM. Optical characterization was carried out on MPc and MPc-GO films using Cary 5000 UV-Vis-NIR spectrophotometer. For the film preparation, necessary amounts of MPc and MPc-GO composites were dispersed in THF for 30 min, then drop-casted on soda-lime glass and dried at RT. The optical band gaps of MPc and MPc-GO composites were determined from analysis of the absorption spectrum through use of Tauc plot, using below Equation (1)<sup>[14,15]</sup>:

$$(\alpha h\nu) = \alpha_0 (h\nu - E_g)^n \quad (1)$$

where  $\alpha$  is absorption coefficient,  $h\nu$  is the energy of the incident photons,  $E_g$  is optical band gap energy (eV) corresponding to the transitions denoted by the  $n$  value, and  $\alpha_0$  is a constant that depends on transition probability.<sup>[14,16,17]</sup>

## 2.3 | Theoretical studies

All calculations were performed using the Perdew-Burke-Ernzerhof (GGA-PBE) exchange-correlation functional and 6-31G(d) electronic basic set using TeraChem software.<sup>[18–23]</sup> Geometry optimization was carried out with the efficient geomeTRIC energy minimizer.<sup>[24]</sup> The dispersion corrections D3 proposed by Grimme were also included to take the weak non-covalent interactions into account.<sup>[25]</sup> Solvent effects were introduced in the frame of the COSMO solvent model.<sup>[26]</sup> The dielectric constant of the solvent (DMSO) was used as 47.2.<sup>[27]</sup> Well-known reactivity parameters like chemical hardness ( $\eta$ ) and electronegativity ( $\chi$ ) are presented as follows<sup>[28,29]</sup>:

$$\mu = -\chi = \left[ \frac{\partial E}{\partial N} \right]_{\nu(r)} = -\left( \frac{I+A}{2} \right) \quad (2)$$

$$\eta = \left[ \frac{\partial^2 E}{\partial N^2} \right]_{\nu(r)} = I - A \quad (3)$$

$$\sigma = \frac{1}{\eta} = \frac{1}{I - A} \quad (4)$$

Softness ( $\sigma$ ) is given as the multiplicative inverse of the hardness while chemical potential ( $\mu$ ) corresponds to the negative value of the chemical hardness. In the given Equations (2)–(4),  $I$  and  $A$  are ground state ionization energy and electron affinity of chemical systems, respectively.  $E$  and  $N$  stand for the total electronic energy and total number of the electrons, respectively.

First electrophilicity index, known as Parr's electrophilicity index, was used in the present work as given below Equation (5)<sup>[30]</sup>:

$$\omega_1 = \frac{\chi^2}{2\eta} = \frac{\mu^2}{2\eta} \quad (5)$$

In the prediction of ionization energy and electron affinities of studied chemical systems, we considered the Koopmans Theorem<sup>[31]</sup> and used the following relations Equations (6) and (7) based on frontier orbital energies:

$$I = -E_{HOMO} \quad (6)$$

$$A = -E_{LUMO} \quad (7)$$

## 3 | RESULTS AND DISCUSSION

Composites of GO with Pc and Pc derivatives are considered to be promising materials for optoelectronic applications because conjugation between functional groups on GO and substituted groups of Pc allow efficient control of charge transport to design materials with enhanced optoelectronic properties. In most cases, the attachment of GO to Pc was reached via covalent bonding. Instead, this research focuses on conjugation of GO and Pc through hydrogen bonding and  $\pi$ - $\pi$  interactions. For this purpose, we first prepared MPc and MPc-GO composites at various compositions as detailed in the experimental section. Sonication time was kept at 5 min to make sure that the interactions between MPc and GO are only via hydrogen bonding and  $\pi$ - $\pi$  stacking.

It is known that UV-Vis is a useful tool to detect intermolecular interactions.<sup>[32]</sup> Thus, the attachment of GO to MPc was studied by UV-Vis spectroscopy as can be seen in Figure 1. The results show that as-prepared MPc shows characteristic Q band of Pcs at 650–750 nm, as expected.<sup>[33–35]</sup> The Q band was split into a doublet of  $Q_x$  and  $Q_y$  with peaks at 686 and 711 nm, respectively, due to the  $D_{2h}$  symmetry of MPc.<sup>[33–35]</sup> We found that the characteristic Q band of MPc was red shifted upon introduction of GO. Also, increase of GO concentration

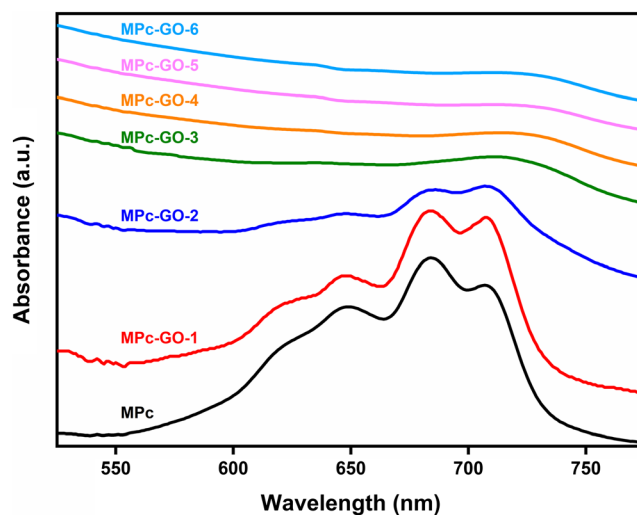


FIGURE 1 UV-Vis absorption spectra of MPc and MPc-GO composites (1: 0.0001  $\mu\text{g/mL}$  GO, 2: 0.001  $\mu\text{g/mL}$  GO, 3: 0.01  $\mu\text{g/mL}$ , 4: 0.05  $\mu\text{g/mL}$  GO, 5: 0.1  $\mu\text{g/mL}$  GO, 6: 1  $\mu\text{g/mL}$  GO).

resulted in a more pronounced red shifting and the disappearance of the doublet until a characteristic single peak was observed at about 732 nm in 9.1 wt.% GO containing composites. Beyond this GO content, further increasing the GO amount did not result in a significant change, thus, suggesting that complete conjugation could be reached at 9.1 wt.% GO. Importantly, these observations strongly suggest that attachment of MPC to GO was via hydrogen bonding. This is because a slight blue shift could normally be expected instead of a strong red shift in case of only  $\pi$ - $\pi$  stacking, as reported by Markad et al.<sup>[12]</sup> Besides, such a red shift might indicate a longer electron delocalization, and thus, indicator of an enhanced charge transport in MPC-GO.<sup>[36]</sup>

The morphologies of resultant MPC-GO hybrids were studied by SEM analysis as shown in Figure 2. Initially, MPC exhibited a pore-free structure with irregularly shaped aggregates. Then, upon introduction of more and more GO, a thinning of MPC was observed and MPC aggregates tended to elongate, eventually resulting in a porous 3d network structure in 9.1 wt% GO containing composites. In fact, this observation might further suggest strong interactions between OH and COOH groups of GO with free NH and N of substituted groups on MPC through hydrogen bonding as schematically illustrated in Figure 2.

Figure 3 compares the FT-IR spectrum of GO, MPC and MPC-9.1 wt.% GO composite. It is known that the region between 4000 and 2500  $\text{cm}^{-1}$  reflects H bonding

and the peaks at about 3600–3200, 3300–3100, and 3300–3000  $\text{cm}^{-1}$  correspond to OH stretching, NH stretching, and CH stretching vibrations, respectively.<sup>[37]</sup> Accordingly, we observed a broad OH peak at about 3500–3200  $\text{cm}^{-1}$  in GO, as expected.<sup>[38]</sup> Also, a strong band belonging to carboxylic acid groups was observed at about 1710  $\text{cm}^{-1}$  in GO, which is consistent with previous reports.<sup>[39]</sup> In case of MPC, only slight peaks were recorded at about 3200 and 3000  $\text{cm}^{-1}$ , and no peak was

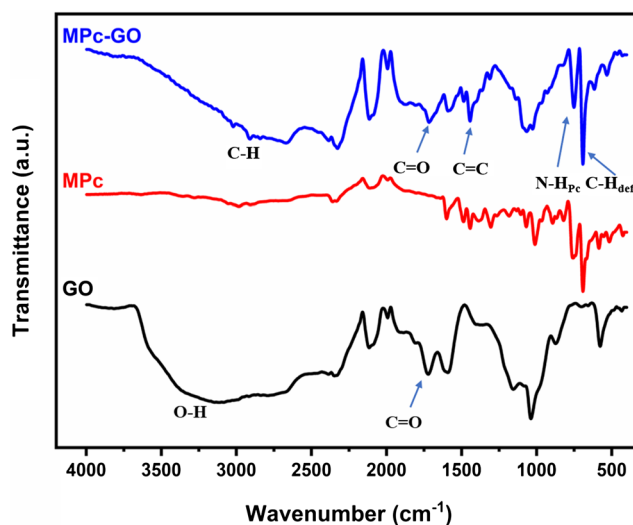


FIGURE 3 Fourier transform infrared (FT-IR) spectra of GO, MPC, and MPC-9.1 wt.% GO composite.

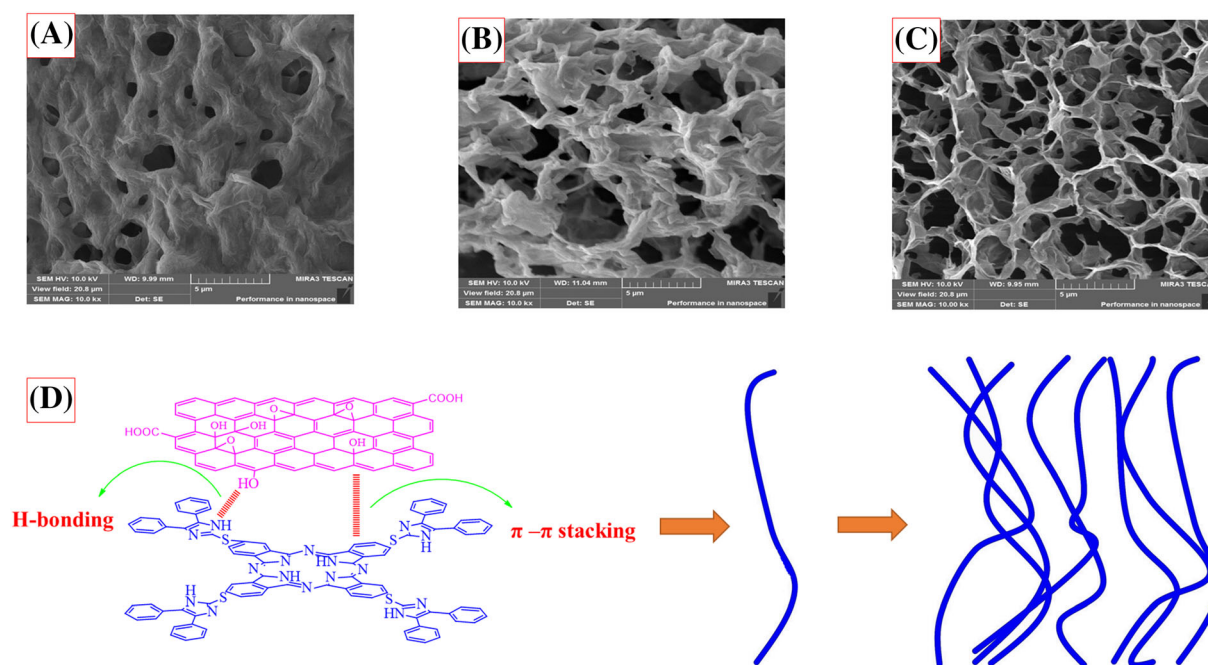


FIGURE 2 Scanning electron microscope (SEM) images of MPC-GO composites (A: MPC-GO-2; B: MPC-GO-4; C: MPC-GO-6). Also, schematic illustration of bonding mechanism in MPC-GO composites (D).



observed at about  $1710\text{ cm}^{-1}$ , which observations are similar with previous reports.<sup>[37]</sup> The slight peaks at about  $3200$  and  $3000\text{ cm}^{-1}$  were ascribed to NH and CH groups of MPc, respectively. Regarding MPc-GO, a decrease of transmittance intensity was observed at about  $3500\text{ cm}^{-1}$ , indicating OH stretching vibration, which could be expected due to the presence of GO. At the same time, the NH peak at about  $3200\text{ cm}^{-1}$  might be masked behind the strong transmittance peak of OH. Yet, a slight peak at about  $3000\text{ cm}^{-1}$  was still observed to some extent in the composite, indicating CH stretching vibrations. Regarding carboxylic acid groups, previous reports indicate that the peak at about  $1710\text{ cm}^{-1}$  disappears in the composite structure when Pc and GO are covalently attached.<sup>[39,40]</sup> However, we still observed this peak in the FT-IR spectrum of MPc-GO, as can be seen in Figure 2, indicating that the attachment of GO to MPc is not through covalent bonding. Also, our observation on a strong intensity drop at the H bonding region in case of MPc-GO is another evidence of strong hydrogen bonding in the composite system. Furthermore, the characteristic bands of MPc were recorded at about  $1596$ ,  $908$ ,  $804$ , and  $749$ , corresponding to C=C, C-N<sub>aza</sub>, N-H<sub>Pc</sub>, and C-H<sub>def</sub>, respectively, all of which are in good accordance with previous reports.<sup>[37]</sup> These bands were also observed in MPc-GO composites, and at almost same wavenumbers. This suggests that there are not significant intramolecular interactions in the composite system, and the main MPc units were intact, further indicating that the incorporation was only through intermolecular hydrogen bonding.

The emission spectra of MPc and MPc-GO composites were illustrated in Figure 4. The emission intensity decreased with increasing GO concentration in composite and the emission peak shifted to lower wavelengths. This indicates more effective energy transfer from phthalocyanine to GO at higher GO concentrations.<sup>[41]</sup> No change was observed in the emission spectra above GO concentration of  $1\text{ }\mu\text{g/mL}$ . This means that optimum GO concentration in this work is  $1\text{ }\mu\text{g/mL}$ , which provides

maximum interaction between GO and MPc. In addition, we investigated the effect of sonication time on the formation of MPc-GO composites. An immediate color change of the solution was observed upon sonication, suggesting rapid conjugation between functional groups of GO and MPc. Also, we report that 5 min is enough to realize a sufficient connection as shown in Figure 4.

Optical properties were studied by UV-Vis through using Tauc plot to comment on the electronic structures and optical transition types of resultant MPc and MPc-GO composites. Particularly, band gap is a vital parameter to determine the potential of a semiconductor for photovoltaic applications. Accordingly, we calculated the optical band gap of as-prepared MPc and MPc-9.1 wt% GO composite by extrapolating the Tauc plot to the abscissa as illustrated in Figure 5.<sup>[14]</sup> According to the graph, the optical band gap of MPc was determined as  $1.77\text{ eV}$ . This result is in good accordance with previous reports on the use of Pc and Pc derivatives in solar cell applications.<sup>[42–45]</sup> Importantly, we report that the optical band gap of MPc-9.1 wt% GO composite is about  $1.57\text{ eV}$ , which makes the composite films even more attractive for photovoltaic applications. This is because the ideal

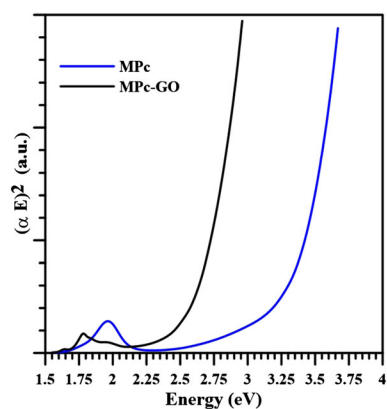
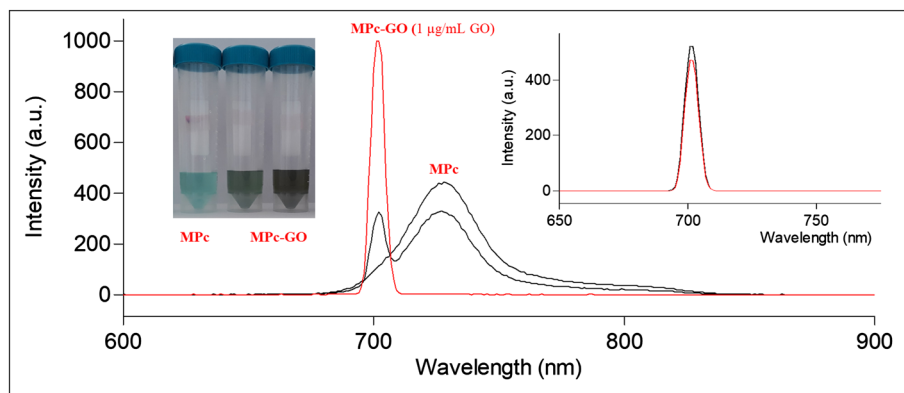


FIGURE 5 Determination of the band gap of MPc-GO hybrid thin film.

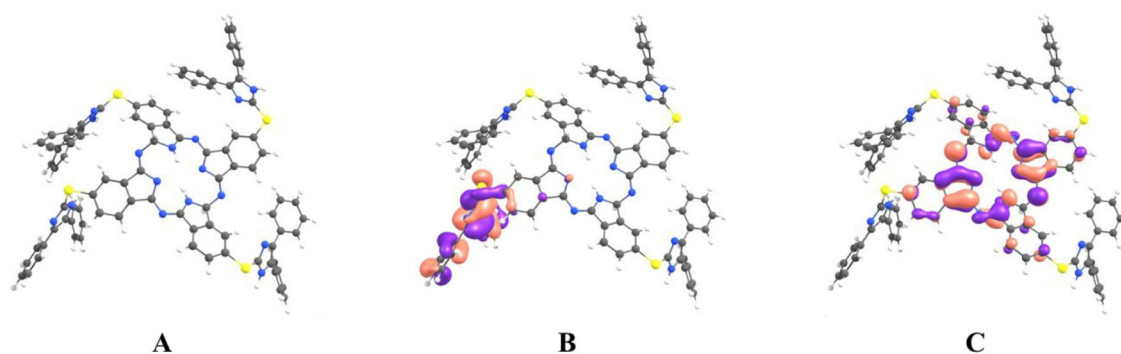
FIGURE 4 Emission spectra of DMSO solution of MPc against different concentrations of GO ( $0\text{ }\mu\text{g/mL}$ ;  $0.05\text{ }\mu\text{g/mL}$ ;  $1\text{ }\mu\text{g/mL}$ ). Emission spectra of MPc-GO composite in DMSO with different sonication times. [Sonication time: 0, 5, 10 min] (top right), color change of MPc and MPc-GO composite solutions with increasing GO amount (top left).



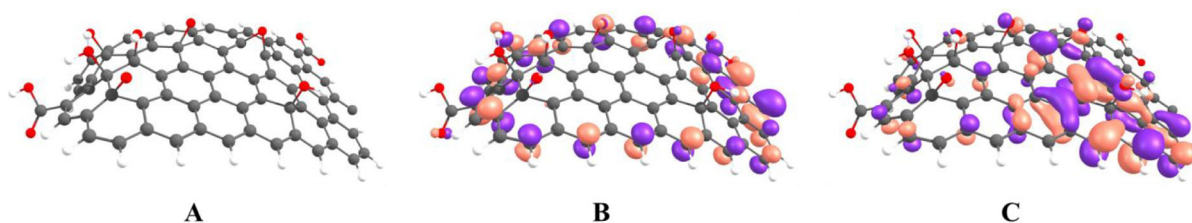
band gap of a semiconductor material is usually considered to be about 1.4 eV for solar cell applications to absorb more photons from sunlight.<sup>[46,47]</sup> Thus, the fact that band gap of MPC-GO is much closer to 1.4 eV suggests that the solar cell performance of MPC might be improved by incorporation of GO to MPC through hydrogen bonding.

After this point, we opted for a theoretical approach to further investigate the effect of hydrogen bonding in the MPC-GO system. All DFT calculations were performed in DMSO media as detailed in the experimental section. The highest occupied molecular orbital (HOMO), lowest unoccupied molecular orbital (LUMO), and optimized geometries, which define the chemical activity and

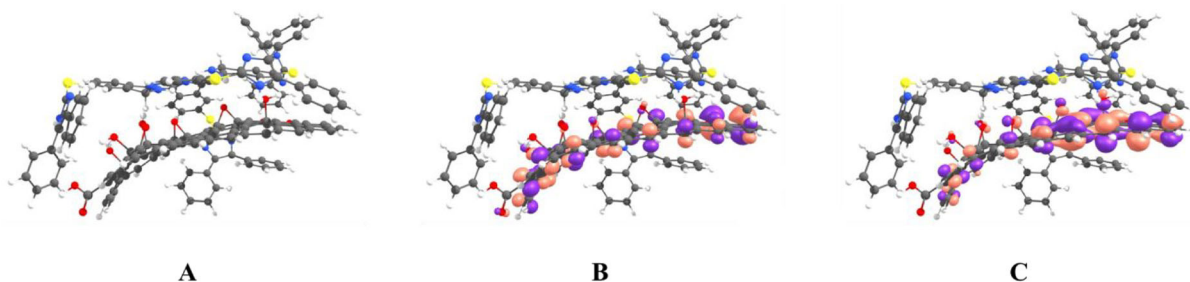
kinetic stability of MPC, GO and MPC-9.1 wt.% GO composite, are shown in Figure 6. The HOMO of MPC is mainly localized on substituted imidazole groups, which might be due to the presence of  $\pi$ -electron sulfur and nitrogen atoms attached to the imidazole ring. Also, the localization of HOMO on imidazole means that the atoms of the main phthalocyanine rings do not contribute much to the charge transfer. Instead, we report that main electron donation could be from the substituted imidazole groups of MPC. Regarding GO, the electron density is concentrated on the bound oxygen and carboxylic acid groups of the conjugate structure. This suggests that there might be strong interactions between substituted imidazole groups of MPC and oxygen



Atomic structure (A), HOMO (B), and LUMO (C) of MPC.



Atomic structure (A), HOMO (B), and LUMO (C) of GO.



Atomic structure (A), HOMO (B), and LUMO (C) of MPC-GO.

FIGURE 6 Optimized geometries, HOMO, and LUMO of MPC, GO, and MPC-9.1 wt.% GO composite.

TABLE 1 Calculated electronic characteristics of studied chemical systems.

Name	Formula	Dipole moment (Debye)	HOMO (eV)	LUMO (eV)	$\chi$ (eV)	$\eta$ (eV)	$\omega_1$ (eV)
MPc	C <sub>92</sub> N <sub>16</sub> H <sub>60</sub> S <sub>4</sub>	7.024	-4.917	-3.105	4.011	1.812	1.812
GO	C <sub>71</sub> H <sub>25</sub> O <sub>11</sub>	8.999	-4.245	-3.938	4.091	0.307	0.307
MPc-GO	C <sub>92</sub> N <sub>16</sub> H <sub>60</sub> S <sub>4</sub> /C <sub>71</sub> H <sub>25</sub> O <sub>11</sub>	10.838	-4.120	-3.793	3.956	0.327	0.327

derivatives of GO in MPc-GO composite structure, which is consistent with theoretical prediction in Figure 6.

The power of the interactions between MPc and GO were studied by theoretical prediction of chemical hardness, dipole moment, softness and electrophilicity index as listed in Table 1. Chemical hardness represents the resistance against polarization of electron cloud.<sup>[48–50]</sup> The inverse relation between hardness and polarizability was highlighted by Ghanty and Ghosh.<sup>[51]</sup> Some researchers emphasized that the dipole moment can be used as a measure of the polarizability. According to Hard and Soft Acid-Base (HSAB) Principle proposed with the help of chemical hardness concept, soft chemical systems interact more powerful with soft chemical systems.<sup>[52]</sup> In the light of the calculated chemical hardness and dipole moment values, it can be said that MPc-GO interaction is a soft-soft interaction, indicating strong interactions between MPc and GO. We calculated the adsorption energy regarding to the interaction between Pc and GO using Equation (8):

$$E_{ads} = E\left(\frac{MPc}{GO}\right) - [E(MPc) + E(GO)] \quad (8)$$

The numerical value of the calculated adsorption energy is -3.153 eV. This value is in good agreement with predictions made via the HSAB Principle. The Maximum Hardness Principle presents the remarkable relation between stability and chemical hardness.<sup>[53]</sup> Within the framework of the mentioned relation, it can be said that hard molecules are stable, while soft chemical systems are reactive.

In optoelectronic applications, the chemical hardness of the materials plays a key role on the resultant performance since chemical hardness is an indicator of charge transfer efficiency.<sup>[54]</sup> In this regard, hard materials exhibit strong resistance to charge transfer, while soft materials are usually preferred in many related applications since they provide better charge transport properties. Our theoretical calculations suggest that charge transport might be more efficient in MPc-GO composites, compared to MPc. This observation is also in good

accordance with our experimental results, which also indicate a decrease in band gap through incorporation of GO to MPc.

## 4 | CONCLUSIONS

There is a considerable research interest on Pc-GO composites for optoelectronic applications. In fact, most previous studies focused on covalent attachment of GO to various Pc derivatives. However, covalent attachment necessitates excessive processing times. On the other hand, hydrogen bonding of functional GO groups to substituted MPc could naturally be much easily realized without harsh reaction conditions. Accordingly, this work aims at investigation of what will happen if MPc-GO composites were prepared via only hydrogen bonding. In this context, it was experimentally observed that imidazole substituted phthalocyanine and GO formed a very stable MPc-GO composite in a very short processing time of only 5 minutes. As-prepared MPc-GO composites were characterized in detail by FT-IR, UV-Vis, SEM, and fluorescence analyses. Also, optical band gaps of MPc and MPc-GO composite were determined from the analysis of the absorption spectrum using the Tauc plot. As a result, the band gap of MPc-9.1 wt.% GO composite was found to be approximately 10% lower than that of MPc. This suggests that MPc-GO composites could absorb more photons from solar radiation, and thus might provide higher energy efficiencies. These findings were also confirmed by theoretical calculations. Overall, it can be said that MPc-GO composites prepared by hydrogen bonding and  $\pi$ - $\pi$  stacking between MPc and GO could provide efficient control of charge transfer. With these properties, hydrogen bonding might be preferred over covalent attachment, particularly when processing times, so does the processing costs, are equally important with the resultant performance.

## ACKNOWLEDGEMENTS

In this study, the laboratory facilities of the Advanced Technology Application and Research Center (CÜTAM) of Sivas Cumhuriyet University were used.

## DATA AVAILABILITY STATEMENT

The data that support the findings of this study are available from the corresponding authors upon reasonable request.

## ORCID

Ebru Yabaş  <https://orcid.org/0000-0001-7163-3057>

Savaş Kaya  <https://orcid.org/0000-0002-0765-9751>

Fuat Erden  <https://orcid.org/0000-0002-8261-4844>

## REFERENCES

- [1] G. Torre, G. Bottari, U. Hahn, T. Torres, *Struct. Bonding* **2010**, *135*, 1.
- [2] K. R. A. Nishida, B. Wiggins, K. W. Hipps, U. Mazur, *J. Phys. Chem. C* **2011**, *115*, 16305.
- [3] M. Yahya, Y. Nural, Z. Seferoğlu, *Dyes Pigm.* **2022**, *198*, 109960.
- [4] E. Yabaş, *J. Austr. Ceramic Soc.* **2022**, *58*, 63.
- [5] A. Ganesan, A. Husain, M. Sebastian, S. Makhseed, *Dyes Pigm.* **2021**, *196*, 109794.
- [6] J. Liang, Z. Lu, Z. Ding, W. Zhang, Y. Li, J. Yu, Y. Wang, P. Li, Q. Fan, *Chem. Eng. J.* **2022**, *435*, 134998.
- [7] G. Lu, P. Zhang, Y. Gao, S. Yu, Y. Yang, *Optics Laser Technol.* **2022**, *149*, 107813.
- [8] R. Ramachandran, Q. Hu, F. Wang, Z. X. Xu, *Electrochim. Acta* **2019**, *298*, 770.
- [9] J. Zhu, Y. Li, Y. Chen, J. Wang, B. Zhang, J. Zhang, W. J. Blau, *Carbon* **1900**, *2011*, 49.
- [10] W. Song, C. He, W. Zhang, Y. Gao, Y. Yang, Y. Wu, Z. Chen, X. Li, Y. Dong, *Carbon* **2014**, *77*, 1020.
- [11] E. Jiang, C. He, X. Xiao, Y. Dong, Y. Gao, Z. Chen, Y. Wu, W. Song, *Opt. Mater.* **2017**, *64*, 193.
- [12] G. B. Markad, N. Padma, R. Chadha, K. C. Gupta, A. K. Rajarajan, P. Deb, S. Kapoor, *Appl. Surf. Sci.* **2020**, *505*, 144624.
- [13] E. Yabaş, M. Sülü, S. Saydam, F. Dumludağ, B. Salih, Ö. Bekaroğlu, *Inorg. Chim. Acta* **2011**, *365*, 340.
- [14] K. J. Hamam, M. I. Alomari, *Appl. Nanosci.* **2017**, *7*, 261.
- [15] M. M. El Nhass, B. S. Sollman, B. S. Metwally, A. M. Farid, A. A. M. Farag, A. A. El Shazly, *J. Opt.* **2001**, *30*, 121.
- [16] H. J. Kim, J. W. Kim, H. H. Lee, B. Lee, J. J. Kim, *Adv. Funct. Mater.* **2012**, *22*, 4244.
- [17] S. Mobtakeri, Y. Akaltun, A. Özer, M. Kılıç, E. Ş. Tüzemen, E. Gür, *Ceram. Int.* **2021**, *47*, 1721.
- [18] J. P. Perdew, K. Burke, M. Ernzerhof, *Phys. Rev. Lett.* **1996**, *77*, 3865.
- [19] M. M. Francl, W. J. Pietro, W. J. Hehre, J. S. Binkley, *J. Chem. Phys.* **1982**, *77*, 3654.
- [20] I. S. Ufimtsev, T. J. Martínez, *J. Chem. Theo. Comp.* **2009**, *5*, 2619.
- [21] A. V. Titov, I. S. Ufimtsev, N. Luehr, T. J. Martínez, *J. Chem. Theo. Comp.* **2013**, *9*, 213.
- [22] J. Kästner, J. M. Carr, T. W. Keal, W. Thiel, A. Wander, P. Sherwood, *J. Phys. Chem. A* **2009**, *113*, 11856.
- [23] T. P. M. Goumans, C. R. A. Catlow, W. A. Brown, J. Kästner, P. Sherwood, *Phys. Chem. Chem. Phys.* **2009**, *11*, 5431.
- [24] L. P. Wang, C. Song, *J. Chem. Phys.* **2016**, *144*, 214108.
- [25] S. Grimme, J. Antony, S. Ehrlich, H. Krieg, *J. Chem. Phys.* **2010**, *132*, 154104.
- [26] F. Liu, N. Luehr, H. J. Kulik, T. J. Martínez, *J. Chem. Theo. Comp.* **2015**, *11*, 3131.
- [27] V. Pilla, A. C. Gonçalves, A. A. Dos Santos, C. Lodeiro, *Chemosensors* **2018**, *6*, 26.
- [28] M. Tuzen, A. Sari, M. R. A. Mogaddam, S. Kaya, K. P. Katin, N. Altunay, *Mater. Chem. Phys.* **2022**, *277*, 125501.
- [29] B. S. Arslan, Y. Derin, B. A. Mısır, S. Kaya, İ. Şişman, A. Tutar, M. Nebioğlu, *J. Molec. Struct.* **2022**, *1267*, 133608.
- [30] R. G. Parr, L. V. Szentpály, S. Liu, *J. Am. Chem. Soc.* **1999**, *121*(9), 1922.
- [31] T. Koopmans, *Physica* **1934**, *1*(1-6), 104.
- [32] T. Hema, T. Bhatt, C. C. Pant, M. Dhondiyal, P. Rana, G. C. J. P. Chowdhury, H. Arya, *J. Mol. Model.* **2020**, *26*, 268.
- [33] G. A. Kumar, G. Jose, V. Thomas, N. V. Unnikrishnan, V. P. N. Nampoori, *Spectrochim. Acta Part a.* **2003**, *59*, 1.
- [34] A. Balliou, J. Pflieger, G. Skoulatakis, S. Kazim, J. Rakusan, S. Kennou, N. Glezos, Programmable molecularnanoparticle multi-junction networks for logic operations, in *NANOARCH '18: IEEE/ACM international symposium on nanoscale architectures, July 17--19, 2018, Athens, Greece* 6 pages, [10.1145/3232195.3232225](https://doi.org/10.1145/3232195.3232225).
- [35] B. W. Caplins, T. K. Mullenbach, R. J. Holmes, D. A. Blank, *J. Phys. Chem. C* **2015**, *119*, 27340.
- [36] H. Y. Yenilmez, B. Ustamehmetoğlu, E. Sezer, Z. Altuntaş-Bayır, *J. Solid State Electrochem.* **2018**, *22*, 505.
- [37] S. Harbecka, Ö. F. Emirik, I. Gürol, A. G. Gürek, Z. Z. Öztürk, V. Ahsen, *Sensor. Actuator. B* **2013**, *176*, 838.
- [38] B. D. Ososon, D. Belanger, *RSC Adv.* **2017**, *7*, 27224.
- [39] P. Kumar, A. Kumar, B. Sreedhar, B. Sain, S. S. Ray, S. L. Jain, *Chem. – Eur. J.* **2014**, *20*, 6154.
- [40] A. H. Aghdam, M. E. A. Araghi, V. Vatanpour, *Phys. E Low Dimens. Syst. Nanostruct.* **2020**, *115*, 113636.
- [41] Z. Zhou, Y. Zhong, M. Xia, N. Zhou, B. Lei, J. Wang, F. Wu, *J. Mater. Chem. C* **2018**, *6*, 8914.
- [42] S. Senthilarasu, S. Velumani, R. Sathyamoorthy, A. Subbarayan, J. A. Ascencio, G. Canizal, P. J. Sebastian, J. A. Chavez, R. Perez, *Appl. Phys. A: Mater. Sci. Process.* **2003**, *77*, 383.
- [43] S. Senthilarasu, R. Sathyamoorthy, S. H. Lee, S. Velumani, *Vacuum* **2010**, *84*, 1212.
- [44] A. Timoumi, M. A. Wederni, N. Bouguila, B. Jamoussi, M. K. A. L. Turkestani, R. Chakroun, B. Al-Mur, *Synt. Metal.* **2021**, *272*, 116659.
- [45] R. R. Kannan, P. I. Nelson, S. Rajesh, T. P. Selvan, A. Mohan, B. Vidhya, D. N. Arivazhagan, *Optic. Mater.* **2018**, *85*, 287.
- [46] Z. L. Yu, Q. R. Ma, B. Liu, Y. Q. Zhao, L. Z. Wang, H. Zhou, M. Q. Cai, *J. Phys. D: Appl. Phys.* **2017**, *50*, 465101.
- [47] O. Polat, M. Çağlar, F. M. Coşkun, M. Coşkun, D. Sobola, Y. Çağlar, A. Turu, *Opt. Mater.* **2020**, *105*, 109911.
- [48] S. Kaya, C. Kaya, *Mol. Phys.* **2015**, *113*(11), 1311.
- [49] S. Kaya, C. Kaya, *Comput. Theoret. Chem.* **2015**, *1060*, 66.
- [50] S. Kaya, A. Robles-Navarro, E. Mejía, T. Gómez, C. Cardenas, *J. Phys. Chem. A* **2022**, *126*(27), 4507.
- [51] T. K. Ghanty, S. K. Ghosh, *J. Phys. Chem.* **1993**, *97*(19), 4951.



- [52] Ş. Berk, S. Kaya, E. K. Akkol, H. Bardakçı, *Phytomedicine* **2022**, *98*, 153938.
- [53] S. Şimşek, Y. Derin, S. Kaya, Z. M. Şenol, K. P. Katin, A. Özer, A. Tutar, *Langmuir* **2022**.
- [54] Y. Li, Y. Li, P. Song, F. Ma, Y. Yang, *J. Mol. Liq.* **2018**, *261*, 123.

**How to cite this article:** E. Yabaş, E. Şenadım-Tüzemen, S. Kaya, M. M. Maslov, F. Erden, *J Phys Org Chem* **2023**, *36*(12), e4496. <https://doi.org/10.1002/poc.4496>